Drag Modulation Flight Control for Aerocapture

Zachary R. Putnam
Georgia Institute of Technology
Atlanta, GA 30332
404-894-7783
zputnam@gatech.edu

Ian G. Clark
Georgia Institute of Technology
Atlanta, GA 30332
404-385-6171
ian.clark@gatech.edu

Robert D. Braun
Georgia Institute of Technology
Atlanta, GA 30332
404-385-6171
robert.braun@aerospace.gatech.edu

Abstract—**Hypersonic deployable aerodynamic devices, both rigid and inflatable, have the potential to enable a broad spectrum of next-generation aeroassist missions by mitigating shape and size constraints on aeroassist vehicles and providing an in-flight reconfiguration capability. Such a capability provides new options for flight control during atmospheric flight, such as drag modulation. Drag modulation is an attractive flight control option for future aerocapture missions because it requires only minimal additional system complexity for vehicles with deployable aerodynamic devices, in contrast to more conventional lift-modulation steering methods. This study expands upon previous aerocapture drag modulation studies by extending the analysis of single-event jettison systems to Earth and Mars. A single-event jettison guidance algorithm was developed and used to evaluate the feasibility of real-time targeting of apoapsis altitude during flight. Results indicate that sufficiently large ballistic coefficient ratios provide adequate aerodynamic and guided corridors for future aerocapture missions. While the preliminary guidance algorithm demonstrates only modest insertion accuracy, this level of accuracy may be tolerable for certain missions.**

TABLE OF CONTENTS

INTRODUCTION

To support the next generation of exploration missions, future aeroassist systems must be able to provide accurate delivery of more massive payloads than systems are currently capable of. This increase in delivered payload mass may be achieved by reducing or eliminating the diameter and shape constraints placed on the aeroassist system by the launch vehicle, allowing the aeroassist vehicle to assume an aerodynamic form that best facilitates mission success. Such deployable aerodynamic devices, both rigid and inflatable, have the potential to enable a broad spectrum of next-generation missions by mitigating shape and size constraints on aeroassist vehicles and potentially providing an in-flight reconfiguration capability. Such a capability provides new options for flight control during atmospheric flight.

978-1-4577-0557-1/12/$26.00 ©2012 IEEE

One such potential option is flight control using drag modulation. Increasing the vehicle drag increases the energy depletion rate and causes the vehicle to drop deeper into a given planetary atmosphere. Decreasing drag has the opposite effect. Therefore, an aeroassist vehicle that can vary its drag is capable of controlling its energy as a function of time, and may therefore control its terminal state. Drag modulation utilizes changes in either vehicle drag area (A) or in drag coefficient (C_D) to change the ballistic coefficient of the vehicle during atmospheric flight to control the vehicle trajectory. Previous studies have examined potential vehicle systems built around both options.

This paper focuses solely on using drag modulation for flight control for aerocapture trajectories, the simplest aeroassist mission targeting problem of interest. Aerocapture provides a simpler targeting problem relative to entry, descent, and landing because no range control is required—only energy must be controlled to achieve the desired terminal state.

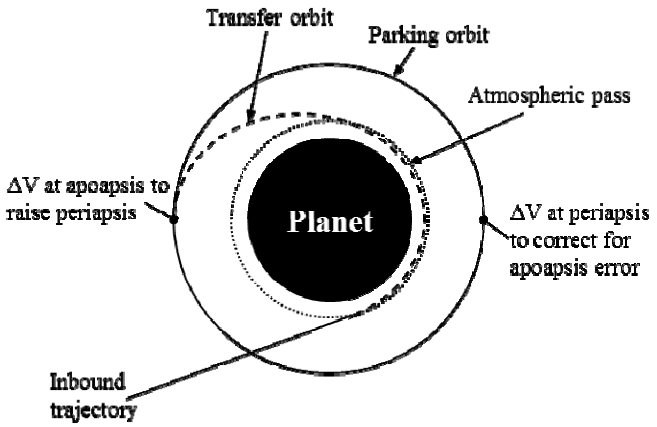

Figure 1 - Aerocapture maneuver to a low parking orbit

The aerocapture maneuver is utilized to transition from a high-energy, possibly hyperbolic, orbit to a lower energy orbit, usually a low parking orbit, without a major propulsive event (see Figure 1). Aerocapture differs from aerobraking in that it depletes the required energy in a single atmospheric pass instead of a series of passes. However, aerocapture still requires some propulsive capability: after the pass, the spacecraft must perform a periapsis raise maneuver at apoapsis to ensure that it does not re-enter the

atmosphere. An additional clean up propulsive maneuver may also be performed at the subsequent periapsis to correct any errors in the apoapsis.

In the early 2000s, a number of studies examined single-event jettison drag modulation systems for aerocapture applications. These systems typically utilized a trailing thin-film ballute to increase drag area. The ballute is deployed prior to atmospheric interface and then jettisoned at the proper time, allowing the spacecraft to coast to the desired state at atmospheric exit. These studies include aerocapture at Titan, Venus, Neptune, and Mars [1][2][3][4]. These studies generally arrive at the conclusion that single-event jettison drag modulation is feasible after solving boundary value problems to determine the time of jettison for a desired atmospheric exit state. However, these conclusions are based solely on the fact that it is physically possible to select a jettison time such that the desired transfer orbit properties are achieved. Two critical areas for feasibility, the feasibility of autonomous, on-board, real-time targeting and robustness to uncertainty are not examined.

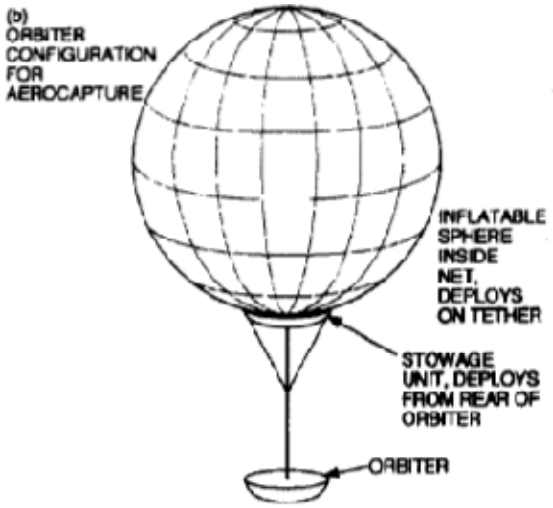

Figure 2 - Trailing thin-film ballute system concept [1]

In the early 1980s, a drag coefficient modulation concept was proposed during the concept definition phase of the development of the Aeroassist Orbit Transfer Vehicle (AOTV), which was to complement the newly built Space Shuttle by ferrying payloads to and from geosynchronous orbit, [5]. The concept, shown in Figure 3, used an inflatable device to increase vehicle drag area and stabilize it during the atmospheric pass and a forward-facing, throttleable chemical rocket engine to modulate overall vehicle CD during the atmospheric pass. Studies of this concept continued until about 1983 when it was abandoned in favor of a more traditional bank-to-steer lift modulation vehicle, which eventually became the Aeroassist Flight Experiment.

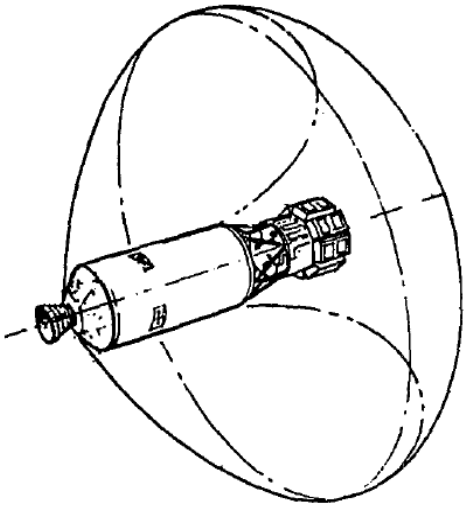

Figure 3 - Drag coefficient modulation AOTV concept [5]

NASA is currently developing technology to mature hypersonic inflatable aerodynamic devices (HIADs) for use in aeroassist vehicles. HIAD vehicles have been featured prominently in recent NASA studies for human Mars exploration [6] and for ISS downmass. While the HIAD development program will likely lead to mature inflatable devices suitable for drag modulation flight control applications in the near future, most studies to date have not considered drag modulation as a flight control option, instead assuming that lift modulation flight control is available, either via bank angle or angle-of-attack modulation. However, for large inflatable vehicles, the dynamic response and effector requirements may make these options infeasible or undesirable. For these types of vehicles, drag modulation presents a simple solution that may provide adequate trajectory control for a variety of aeroassist missions. Drag modulation is particularly attractive for aerocapture trajectories, as the absence of out-of-plane control authority may be less important than for entry, descent, and landing systems.

The goal of this study is to determine the feasibility of drag modulation for aerocapture missions. Assessment of feasibility involves three major analyses:

(1) Ensuring that the flight-path angle corridor can accommodate current navigation capabilities
(2) Determining the feasibility of real-time targeting
(3) Determining system robustness to uncertainty

This study seeks to determine the feasibility of drag modulation flight control through the completion of these analyses for single-event jettison drag modulation systems.

The remainder of this paper is organized in the following manner. Section 2 provides detailed information on the numeric trajectory simulation and models used for the analyses presented in this paper, as well as analysis assumptions. Section 3 discusses system-level capability and performance results for drag modulation vehicles.

Section 4 provides detail on the feasibility of single-event jettison drag modulation systems. Conclusions are provided in Section 6.

ASSUMPTIONS AND SIMULATION

Assumptions

The analyses presented in this paper utilize numeric simulation of the equations of motion for aerocapture. For the purposes of this study, the ballistic coefficient, β, is given by

$$\beta = m/C_D A$$

where m is the vehicle mass, C_D is hypersonic drag coefficient at Mach 25, and A is the aerodynamic reference area.

Unless otherwise noted, the vehicle state at atmospheric interface for the trajectories in this paper is given in Table 1. Flight-path is defined as the angle between the local horizontal and the velocity vector, with positive angles above the horizon. Azimuth is defined to be degrees east of north. While atmospheric interface is typically defined at 125 km altitude for the Earth and Mars, a value of 150 km was adopted to ensure accurate simulation for the low ballistic coefficient vehicles considered in this study.

Table 1. Atmospheric Interface State

State Parameter	*Value*
Geodetic altitude	150 km
Geodetic latitude	0 deg
Longitude	0 deg
Inertial velocity magnitude	Varies
Inertial geocentric flight-path	Varies
Inertial geocentric azimuth	90 deg

Trajectory Simulation

A three-degree-of-freedom numeric simulation developed at the Space Systems Design Lab at Georgia Tech was used to determine aerocapture flight performance for this study. The equations of motion are integrated using a fourth order Runge-Kutta scheme with a constant time step of 0.01s. This scheme provides a good balance between accuracy and computational cost. The simulation is written in Matlab m-code to maintain portability, and may be autocoded and compiled to improve execution speed.

Vehicle Models—Vehicle hypersonic aerodynamics were modeled as 60 deg sphere cones for Earth and 70 deg sphere cones for Mars, both flying at a trim angle of attack of zero. Drag modulation was achieved through changing the aerodynamic reference area. The mass change from jettisoning drag surfaces was assumed to be negligible, and no separation dynamics were modeled. Navigation was assumed to be perfect.

Environment Models—The Earth and Mars were modeled as ellipsoids, based on their equatorial and polar radii. Planetary gravity was modeled as an inverse square magnitude with J_2 effects. Planetary atmospheres were modeled with tables of density and temperature as a function of altitude. Atmospheric table data were generated with Earth-GRAM 2010 Version 2 [7] and Mars-GRAM 2010 [8] for Earth and Mars, respectively.

Uncertainty Analysis—Monte Carlo techniques were used to assess robustness to uncertainty. Distributions were assigned to inputs of interest, including atmospheric density, vehicle aerodynamics, and initial vehicle state, and sets of distributed inputs were generated for use with the numeric simulation. Uniform and normal distributions were used, as appropriate.

SYSTEM CAPABILITY AND PERFORMANCE

Flight-path Corridor Identification

The flight-path angle corridor is defined as the range of flight-path angles at atmospheric interface for which the vehicle can reach the desired atmospheric exit conditions. For aerocapture trajectories, this terminal condition translates to achieving a particular apoapsis altitude at atmospheric exit. For drag modulation systems, the flight-path angle corridor is bounded by the minimum and maximum drag configurations of the vehicle, by whatever means those configurations are achieved. The steepest initial flight-path angle for which the lowest drag, highest ballistic coefficient, trajectory can reach the desired apoapsis altitude defines the steep side of the corridor. The shallowest initial flight-path angle for which the highest drag, lowest ballistic coefficient vehicle can reach the desired apoapsis altitude defines the shallow side of the corridor.

Figure 4 below shows the bounding trajectories for an example vehicle performing aerocapture at Earth with a 400 km apoapsis altitude target. This vehicle has a mass of 1000 kg and enters the atmosphere at an inertial velocity magnitude of 10 km/s. This vehicle is capable of changing its drag area to vary its ballistic coefficient between 10 and 100 kg/m^2. The plot in (a.) clearly shows the shallow bounding trajectory in blue and the steep bounding trajectory in red. The sensed deceleration profiles are also shown in (b.). Notice that, while the low-β trajectory decelerates higher in the atmosphere where density is low, it experiences a slightly higher peak deceleration than the high-β trajectory.

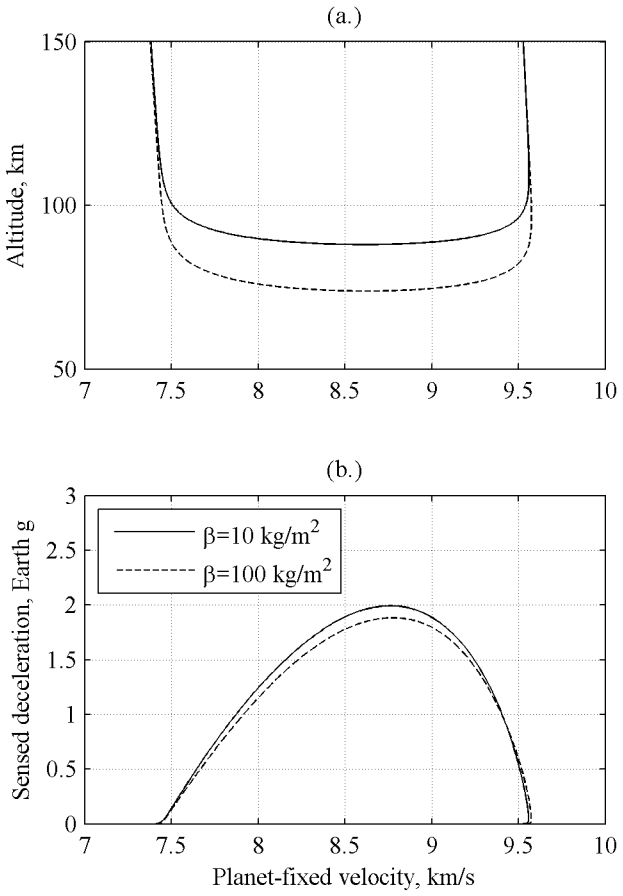

Figure 4 – Corridor-bounding trajectories for aerocapture at Earth: (a.) altitude and (b.) deceleration

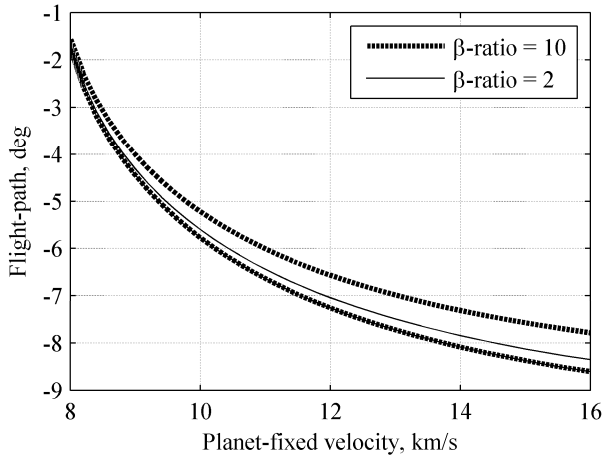

Figure 5 - Flight-path angle corridor at Earth

The flight-path corridor can be determined over a range of velocities. Figure 5 shows the flight-path corridor for aerocapture at Earth to an apoapsis altitude of 400 km for the same vehicle discussed above. This plot shows the corridor for a range of velocities spanning low-Earth orbit to free-return Mars trajectories. The corridor steepens and widens with increasing velocity. Most importantly, this plot shows that there is a non-zero width corridor over a wide range of entry velocities, indicating that drag modulation is potentially useful for a wide range of aerocapture missions.

Corridor Variation

The variation of the flight-path corridor with respect to several parameters was examined to determine which parameters are most important for mission and guidance, navigation, and control system design.

Apoapse Target Variation—The flight-path corridor was determined for several apoapsis target altitudes from 200 km to 1200 km in 200 km increments. Results are shown below in Figure 6 for Earth and indicate that the corridor width and position are essentially invariant with respect to target apoapsis altitude.

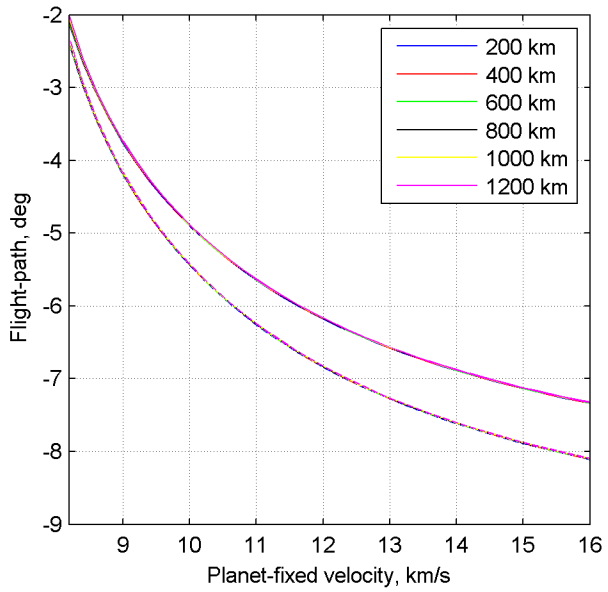

Figure 6 - Flight-path corridor as a function of velocity for several apoapsis altitude targets at Earth

β-ratio and β Magnitude Effects—The effects of different β-ratios and β magnitudes on the flight-path corridor were examined. Results at Earth are shown in Figure 7 and Figure 8, respectively. Increasing the β-ratio has a significant impact on corridor width, with a β-ratio of 10 providing over three times the width of a β-ratio of 2. Increasing the magnitude of β only slightly increases the corridor width, with greater effects at higher velocities. As expected, increasing the magnitude of β also steepens the corridor. These figures show that β-ratio is the strongest indicator of corridor width. The magnitude of β determines the corridor position but has only a second-order effect on corridor width.

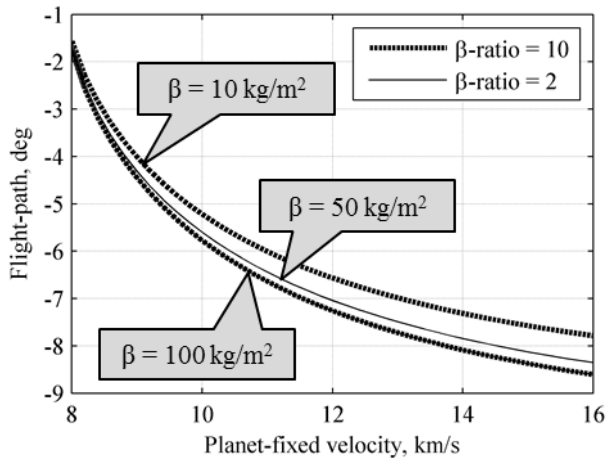

Figure 7- Flight-path angle corridor at Earth for two different β-ratios

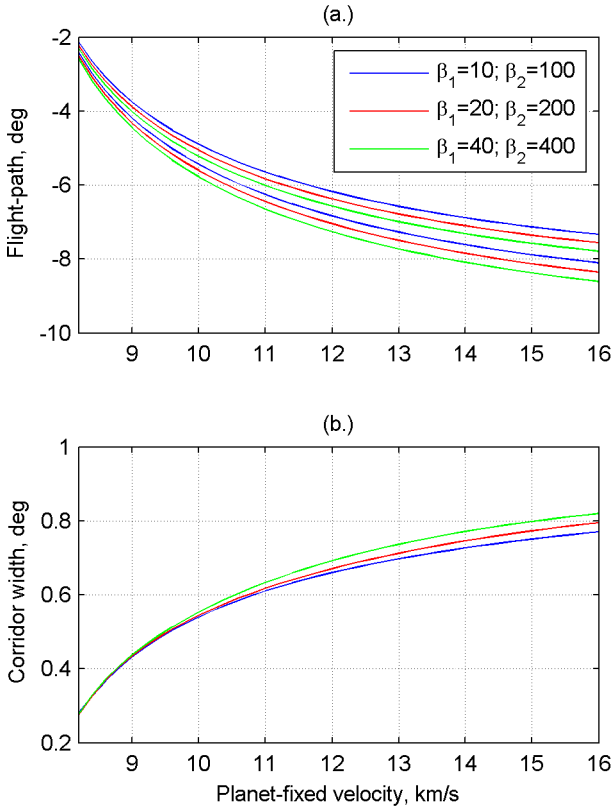

Figure 8 - Flight-path corridor (a.) and width (b.) for several β magnitudes at Earth

SINGLE-EVENT JETTISON SYSTEMS

The previous section showed that a non-zero corridor exists at Earth for drag modulation systems. However, one must be able to effectively target the desired apoapse altitude in real-time during aerocapture from an arbitrary position within the flight-path corridor. One flight control option is single-event jettison drag modulation.

Concept Overview

Single-event jettison drag modulation relies upon a single change in drag area during the atmospheric pass to target the desired apoapsis altitude. While many flight systems can be envisioned which have the capability to change their drag area, a simple example of this type of system is that given by a spacecraft with an attached inflatable device. For the purposes of this paper, the attached inflatable device is assumed to approximate a 60-deg sphere cone at Earth and a 70-deg sphere cone at Mars. At the proper time, the inflatable device is jettisoned, thereby changing the drag area and ballistic coefficient of the vehicle.

The proper jettison time is determined in real time by and on-board guidance algorithm. The algorithm uses the current vehicle state and the desired final state to determine when the inflatable device should be jettisoned at each guidance call during flight. When the jettison time is reached, the guidance algorithm sends the command to the vehicle to jettison the inflatable device.

Guidance Algorithm Development

A basic guidance algorithm was developed to facilitate the analyses in this paper. A numeric predictor-corrector (NPC) was chosen for the algorithm due to its ease of implementation and conceptual simplicity.

A summary block diagram of the algorithm is shown in Figure 9. The vehicle state is passed to guidance from navigation, assumed to be perfect for this study, and some preliminary calculations are conducted prior to continuing to the proper mode. The required input state variables are given in Table 2. Initially, the algorithm waits in a hold until the drag acceleration builds to 0.5 m/s^2. At that point, the algorithm transitions to the numeric predictor-corrector targeting phase. The NPC computes the proper time for jettison and passes it to the jettison logic. The jettison logic then determines whether it is time to perform the jettison. If it is time to perform the jettison, a jettison command flag is passed to flight control. Once jettison has occurred, the algorithm transitions to a second hold phase until atmospheric exit.

The NPC runs the predictor and corrector in a loop, limited to five iterations per guidance cycle. If a solution for the jettison time is not found on a given guidance cycle, the algorithm stores its current best estimate and continues on subsequent guidance cycles with updated navigation inputs. The guidance algorithm is called every 2 seconds during the atmospheric pass.

The NPC also estimates the current atmospheric density from the navigated acceleration and determines a density scale factor which is applied to the on-board atmosphere model during prediction. The current density is estimated from

$$\rho = \frac{2ma_{mag}}{V_{rel}^2 S_{ref} C_D}$$

The estimation assumes a constant, known hypersonic drag coefficient. The density factor is simply the ratio of the

estimated density to the on-board model density at the current altitude. The density factor estimate is also run through a low-pass filter to reduce oscillation.

Predictor—The numeric predictor integrates the equations of motion forward in time from the current vehicle state to atmospheric exit. It uses a variable step size, 4th order Runge-Kutta integration scheme. The predictor nominally runs at a step size of 2 seconds, but this step size is decreased to the minimum jettison time adjustment increment near jettison time to ensure that jettison is modeled properly. After jettison, the step size returns to its nominal value. This reduction in step size is critical due to the extreme sensitivity of the final vehicle state to jettison time. Constant hypersonic aerodynamics was assumed for the spacecraft, and was assumed to scale only with aerodynamic reference area. The attracting planet is modeled as a sphere with inverse-square gravity and J2 effects. Atmospheric density is modeled by a table of density versus altitude.

Corrector—The corrector uses the estimated final state from the predictor to adjust the jettison time to reduce the apoapsis altitude error to within a specified tolerance. If the estimated final apoapsis is too high, the jettison time is adjusted to occur later in the trajectory; if the estimated final apoapsis is too low, the jettison time is adjusted to occur earlier in the trajectory. If a sign change is detected in the apoapsis error, the jettison time adjustment increment is reduced by 50%, subject to a minimum allowable increment. If the predicted apoapsis is negative, indicating a hyperbolic trajectory at atmospheric exit, the corrector marches towards the capture region by increasing the jettison time with a large increment.

Table 2. Guidance Algorithm Inputs

Name	*Units*	*Description*
t	s	Reference time
R_pci	m	Vehicle position vector in planet-centered inertial frame
V_inrtl_pci	m/s	Vehicle inertial velocity vector in planet-centered inertial frame
A_asens_pci	m/s^2	Vehicle sensed acceleration vector in planet-centered inertial frame

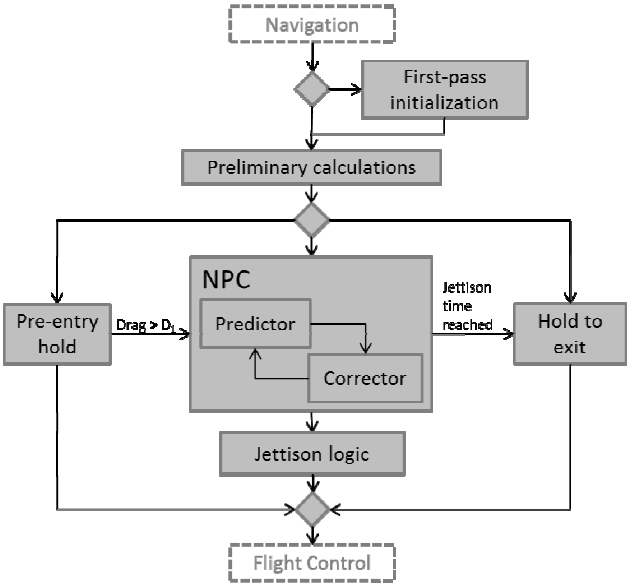

Figure 9 - Single-event jettison guidance algorithm block diagram

An example guided single-event jettison aerocapture trajectory is shown in Figure 10. The vehicle enters the atmosphere at 10 km/s inertial velocity magnitude and jettisons the inflatable device at 119.81 s. At this point, there is a discontinuity in the trajectory as the vehicle ballistic coefficient changes from 10 kg/m2 to 100 kg/m2 instantly. The sensed deceleration immediately decreases and the vehicle begins to descend farther into the atmosphere. While the drag level does increase somewhat from its post-jettison value, it remains below one Earth g for the remained of the trajectory. Figure 11 shows the apoapsis altitude at atmospheric exit during the trajectory as it would be if the spacecraft exited the atmosphere at that point. The decrease in the apoapsis altitude to the target value indicates that the guidance algorithm has effectively timed the jettison to achieve the target exit condition.

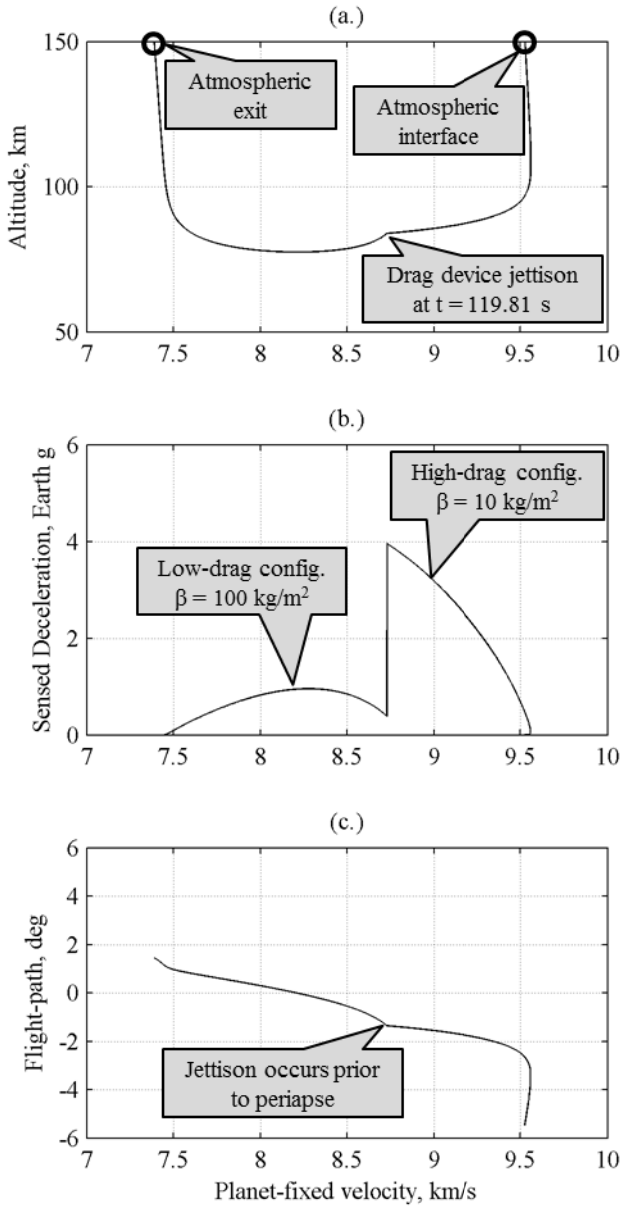

Figure 10 - Sample guided aerocapture trajectory at Earth

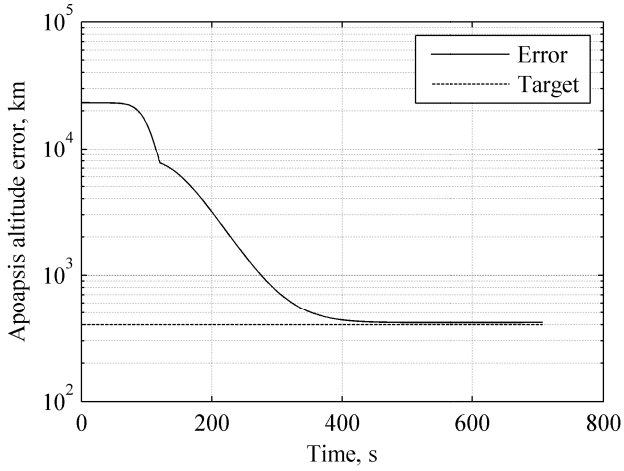

Figure 11 - Apospasis error during aerocapture at Earth

Jettison Time Sensitivity

During guidance algorithm development, it was noticed that the vehicle was extremely sensitive to the jettison time. A brief analysis was conducted to identify the magnitude of the sensitivity. Figure 12 shows the sensitivity of the final apoapsis altitude with respect to jettison time, dh_a/dt_j over a range of jettison times for an inertial entry velocity of 11 km/s at several initial flight-path angles at Earth. Early in the trajectory, the sensitivity is low or zero due to low drag. However, once drag builds to a sufficient level, a jettison time lag or error of just 1 second can change the final apoapse altitude by hundreds of kilometers, possibly resulting in a surface impact.

In many early guidance test cases, the algorithm failed to achieve the desired target apoapsis altitude due to this sensitivity and the relatively slow guidance execution rate of 0.5 Hz. However, because the numeric prediction algorithm is relatively computationally intensive, increasing the guidance execution rate was not a desirable solution. Instead, a variable time-step integration scheme was added to the predictor, and the jettison logic was pulled out of the numeric predictor-corrector phase such that it was executed at a higher rate than the rest of guidance. These two changes significantly improved accuracy while preserving the 0.5 Hz guidance rate.

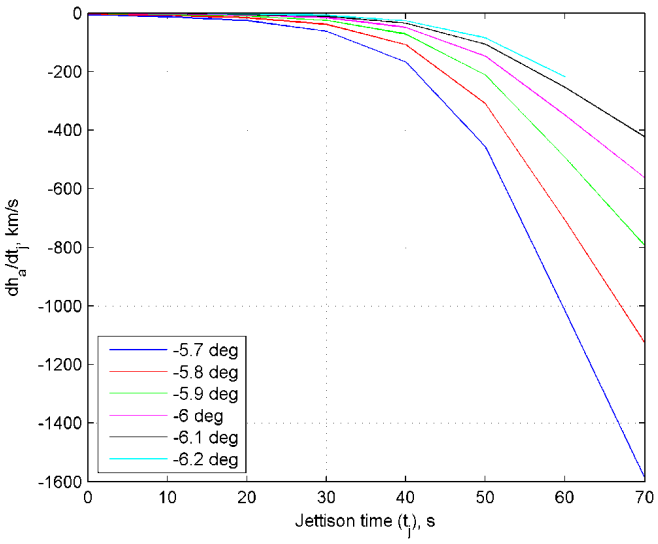

Figure 12 - Sensitivity of final apoapsis altitude to jettison time at Earth at 11 km/s

Guided Flight-path Corridor

The developed guidance algorithm was used to evaluate the guided flight-path angle corridor at Earth and Mars for a vehicle with a β-ratio of 10, similar to the vehicle used in other corridor analyses presented in this study. The apoapsis altitude target for these corridors is 400 km. Figure 13 and Figure 14 show the guided flight-path angle corridor as a function of inertial entry velocity magnitude at the Earth and Mars, respectively. The plots show the guided corridor in orange. Dark blue indicates the undershoot region. The

white region in the lower left corner indicates surface impact. The blue region is very narrow because there is only a small range of possible apoapsis altitudes available below the target altitude of 400 km before the vehicle does not exit the atmosphere and impacts the planetary surface. The red region indicates overshoot and the white region in the upper right corner indicates overshoot or hyperbolic exit conditions.

The primary conclusion from these plots is that the guided corridor is nearly the same size as the aerodynamic corridor developed in Section 3. This indicates that the guidance algorithm is effectively using the vehicle's capability to achieve the desired target throughout the corridor over a wide range of velocities and that vehicle is flyable over most of the aerodynamic corridor. The plots also show that apoapsis target accuracy falls off quickly to either side of the corridor. Accuracy also deteriorates within the corridor for higher-energy trajectories.

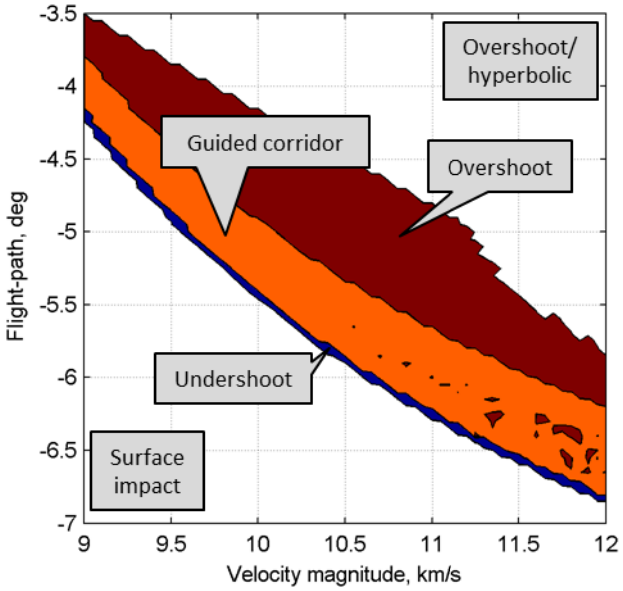

Figure 13 - Guided flight-path corridor at Earth for single-event jettison configuration

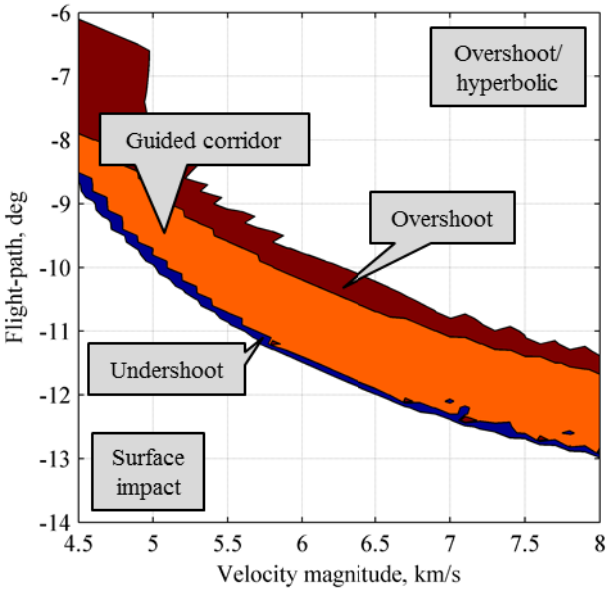

Figure 14 - Guided flight-path corridor at Mars for single-event jettison configuration

Uncertainty Analysis

Uncertainty analysis was also performed for two representative test cases, one at Earth and one at Mars. Both cases utilized a vehicle with an initial β of 10 kg/m^2 and a final β of 100 kg/m^2, resulting in a β-ratio of 10. The initial aerodynamic reference area is 200 m^2. After jettison, the reference area is 20 m^2. For these properties, the resulting mass of the vehicle was calculated to be 3060 kg. The nominal atmospheric interface states at Earth and Mars are given in Table 3. The Earth atmospheric interface state corresponds to that which might be seen by a space tug returning a payload to low-Earth orbit, similar to that of the original design mission for the AOTV. The Mars state corresponds to one which might be seen by a spacecraft attempting to enter orbit around Mars upon arrival from Earth.

Table 3. Nominal Atmospheric Interface States

State Parameter	*Earth*	*Mars*
Geodetic altitude	150 km	150 km
Geodetic latitude	0 deg	0 deg
Longitude	0 deg	0 deg
Inertial velocity magnitude	10 km/s	6 km/s
Inertial geocentric flight-path	-5.2 deg	-10.8 deg
Inertial geocentric azimuth	90 deg	90 deg

A Monte Carlo simulation was conducted with dispersions applied to the initial vehicle state, vehicle aerodynamics, and planetary atmosphere. 500 samples were used to determine apoapsis altitude accuracy for a 400 km altitude target. Table 4 shows the apoapse accuracy for both cases. Histograms of the apoapsis altitude accuracy are shown in Figure 15 and Figure 16 for the Earth and Mars cases, respectively. The algorithm is able to guide the vehicle

effectively for nearly all samples. The Mars case has one outlier with a nearly 1000 km overshoot. This case significantly increases the standard deviation; when the outlier is eliminated, the standard deviation is less than 15 km. This indicates a similar level of accuracy for both Earth and Mars when outliers are neglected. While this level of accuracy is not as good as can be provided with a lifting system, it indicates that drag modulation may be a feasible option when precision orbital insertion is not critical. Additionally, accuracy may be improved with improvements to the algorithm, including higher fidelity prediction and better density or drag estimation techniques.

Table 4. Apoapse Accuracy at Atmospheric Exit

Parameter	*Earth*	*Mars*
Mean	25.9 km	-3.45 km
Standard deviation	15.2 km	45.7 km
Minimum	-65.6 km	-78.4
Maximum	68.5 km	974 km

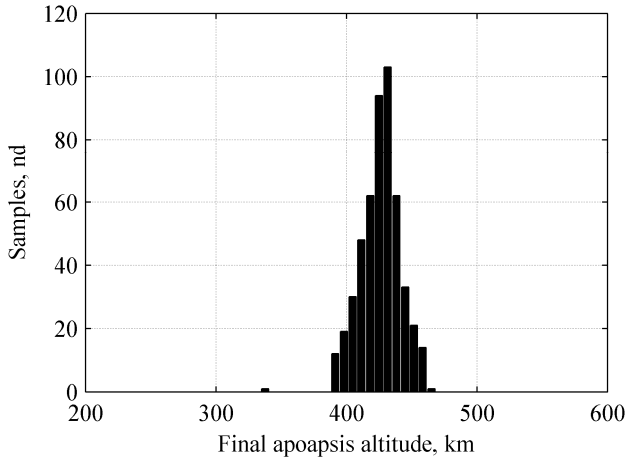

Figure 15 - Final apoapsis altitude at Earth for a nominal velocity and flight-path of 10 km/s and -5.2 deg

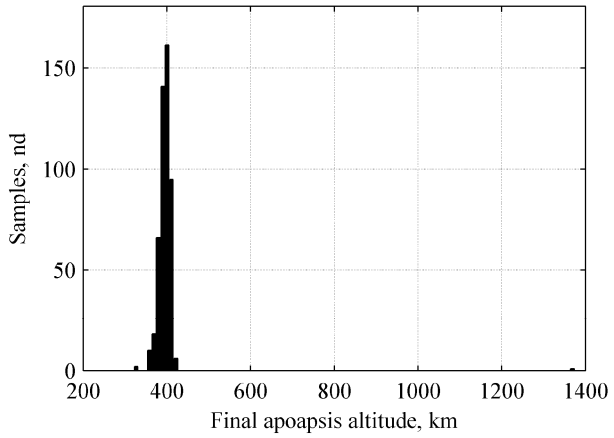

Figure 16 - Final apoapsis altitude at Mars for a nominal velocity and flight-path of 6 km/s and -10.8 deg

CONCLUSIONS

In conclusion, it has been shown that sufficient ballistic coefficient ratios provide a flight-path corridor over a wide range of velocities at the Earth and Mars that can accommodate current approach navigation uncertainties. Furthermore, a prototype numeric predictor-corrector guidance algorithm was developed to perform targeting for single-event jettison drag modulation systems. This algorithm was used to show that the guided single-event jettison corridor is nearly the same size as the aerodynamic corridor at the Earth and Mars. Uncertainty analyses performed with Monte Carlo techniques show that drag modulation may be a viable flight control technique when precision orbital insertion is not critical.

ACKNOWLEDGEMENTS

This work was supported by a NASA Office of the Chief Technologist's Space Technology Research Fellowship.

REFERENCES

[1] McRonald, Angus, D., "A Light-weight Inflatable Hypersonic Drag Device for Venus Entry," AAS 99-355, AAS/AIAA Astrodynamics Specialist Conference, Girdwood, AK, 16-19 August 1999.

[2] McRonald, Angus D., "A Light-weight Hypersonic Inflatable Drag Device for a Neptune Orbiter," AAS 00-170, AAS/AIAA Space Flight Mechanics Meeting, Clearwater, FL, 23-26 January 2000.

[3] Hall, Jeffery L., Le, Andrew K., "Aerocapture Trajectories for Spacecraft with Large, Towed Ballutes," AAS 01-235, AAS/AIAA Space Flight Mechanics Meeting, Santa Barbara, CA, 11-14 February 2001.

[4] Westhelle, Carlos H., Masciarelli, James P., "Assessment of Aerocapture Flight at Titan Using a Drag-only Device," AIAA 2003-5389, AIAA Atmospheric Flight Mechanics Conference and Exhibit, 11-14 August 2003, Austin, TX.

[5] Andrews, D.G, Bloetscher, F., "Aerobraked Orbital Transfer Vehicle Definition," AIAA-81-0279, AIAA 19th Aerospace Sciences Meeting, 12-15 January 1981, St. Louis, MO.

[6] Dwyer, Alicia M., et. al., "Entry, Descent and Landing Systems Analysis Study: Phase 1 Report," NASA/TM-2010-216720, July 2010.

[7] Leslie, F.W., Justus, C.G., "The NASA Marshall Space Flight Center Earth Global Reference Atmospheric Model—2010 Version," NASA/TM-2011-216467, June 2011.

[8] Justus, C.G., Johnson, D.L., "Mars Global Reference Atmospheric Model 2001 Version (Mars-GRAM 2001): Users Guide," NASA/TM-2001-210961, April 2001.

BIOGRAPHIES

Zachary R. Putnam *is a doctoral student in aerospace engineering in the Space Systems Design Lab at the Georgia Institute of Technology and a NASA Space Technology Research Fellow. His research focuses on guidance and control systems and mission design for aeroassist vehicles. He was previously a member of the technical staff at the Charles Stark Draper Laboratory, where he supported development of the Orion entry guidance system. Mr. Putnam received his B.S. and M.S. in Aerospace Engineering from the Georgia Institute of Technology.*

Ian G. Clark *is a visiting assistant professor at the Georgia Institute of Technology and an employee of the Jet Propulsion Laboratory. He received his PhD from the Georgia Institute of Technology, where he also received his BS and MS. Ian's current research involves developing and maturing IADs for use during atmospheric entry. As part of this research, Dr. Clark has worked on conceptual IAD system design, entry flight mechanics trades, and the development of fluid- structure interaction codes capable of predicting the behavior of flexible decelerators.*

Robert D. Braun *is the David and Andrew Lewis Professor of Space Technology in the Daniel Guggenheim School of Aerospace Engineering at the Georgia Institute of Technology. As Director of Georgia Tech's Space Systems Design Laboratory, he leads a research program focused on the design of advanced flight systems and technologies for planetary exploration. He is responsible for undergraduate and graduate level instruction in the areas of space systems design, astrodynamics, and planetary entry. He served as NASA's Chief Technologist in 2010 and 2011. Prior to coming to Georgia Tech, he served on the technical staff of the NASA Langley Research Center, where he contributed to the design, development, test, and operation of several robotic space flight systems. Dr. Braun is an AIAA Fellow and holds a B.S. in Aerospace Engineering from Penn State University, a M.S. in Astronautics from George Washington University, and a Ph.D. in Aeronautics and Astronautics from Stanford University.*